

REGULAR PAPER

Pulse light manipulate output state of 3.6 μm fluoride fiber laser in DWP system

To cite this article: Xin Zhang *et al* 2022 *Jpn. J. Appl. Phys.* **61** 082005

View the [article online](#) for updates and enhancements.

You may also like

- [Mask-free patterning and selective CVD-growth of 2D-TMDCs semiconductors](#)
Dheyaa Alameri, Joseph R Nasr, Devon Karbach et al.
- [Comparison of ionisation chamber and semiconductor detector devices for measurement of the dose-width product for panoramic dental units](#)
S A Mitchell and C J Martin
- [Approximate inverse Ising models close to a Bethe reference point](#)
Cyril Furtlehner



Pulse light manipulate output state of 3.6 μm fluoride fiber laser in DWP system

Xin Zhang¹, Cunzhu Tong^{1,*}, Kaidi Cai^{1,2}, and Yanjing Wang¹¹State Key Laboratory of Luminescence and Applications, Changchun Institute of Optics, Fine Mechanics and Physics, Chinese Academy of Sciences, Changchun 130033, People's Republic of China²Center of Materials Science and Optoelectronics Engineering, University of Chinese Academy of Sciences, Beijing 100049, People's Republic of China*E-mail: tongcz@ciomp.ac.cn

Received May 10, 2022; revised June 14, 2022; accepted June 28, 2022; published online July 22, 2022

Strong driving with light offers the potential to manipulate the properties of fluoride fiber on absorbed characteristics. A 3.6 μm continuous wave (CW) fiber laser pumped by the 1973 nm CW fiber laser and the 976 nm pulsed diode source was demonstrated in a dual-wavelength pumping (DWP) system. The output state could be changed from pulse to CW by controlling the repetition frequency and pumping power of the 976 nm pulsed pump source. By optimizing the pumping parameter, a maximum output power of 1.2 W was achieved for the 3.6 μm CW fiber laser. The demonstrated method shows a new solution for controlling the output state of 3.6 μm fiber lasers, which can be used to achieve high power CW laser output. These findings will be helpful for better understanding the interaction process of particle transition in DWP systems.

© 2022 The Japan Society of Applied Physics

1. Introduction

There is an increasing scientific interest in developing laser sources at mid-infrared wavelengths to fulfill various application needs in the biomedical,^{1–3)} defense and security,^{4–6)} material processing.^{7–9)} In particular, 3.5 μm waveband fluoride fiber lasers have become a research hotspot due to their good beam quality, high brightness and transparency in an atmospheric window.^{10–12)} In order to improve 3.5 μm laser slope efficiency, the method of dual-wavelength pumping (DWP) was proposed by Henderson-Sapir et al.¹³⁾ Since then, the output power was constantly refreshed through continuous optimization of laser design.^{14–17)} Meanwhile, the methods of pulsed modulation, such as Gain-switched,^{18–20)} active Q-switched,²¹⁾ passively Q-switched^{22–24)} and mode locked^{25–28)} were also investigated in the DWP system. However, the states of the 976 nm pump source reported in the literature were all continuous wave (CW). The main function of the 976 nm pump source was to provide enough erbium ions to the metastable energy level to meet the 1973 nm pumping demand. If the 976 nm pulsed pump source was adopted in the DWP system, the erbium ions on metastable energy level would be changed with the time so that the state of output would be manipulated by varying the repetition rate and the duty cycle. Moreover, the heat distribution in the system would also be changed. Therefore, it is of great significance to study the influence of pulse pumping on the 3.6 μm fiber laser system for a better understanding of the interaction process of particle transition in the DWP system.

In this paper, the pulse pumping was proposed to achieve a 3.6 μm CW fluoride fiber laser in the DWP system. The output time envelope under different repetition frequencies of 976 nm pulsed pump was compared, with the output spectrum and power measured simultaneously. Finally, the corresponding theory of pulse pumping was also discussed at the end of the paper.

2. Experimental setup

The setup for the experiment is shown in Fig. 1. The gain fiber was 3.8 m in length and 1.5 mol.% concentration erbium-doped fluoride (Er:ZBLAN) fiber. The diameter and numerical aperture of the fiber core were 16.5 μm and 0.12, respectively. Its 260 μm cladding had a circular shape with two parallel flats separated by

240 μm . The 976 nm fiber-coupled diode laser and 1973 nm fiber laser were used as pump sources. The chopper was used to change the mode of the 976 nm pump source from CW to pulse. The 1973 nm pump source was a homemade Tm doped single-mode fiber laser. Double pump sources were combined by a Dichroic mirror (DM) and then coupled into the Er:ZBLAN fiber. The focus length of lenses L1 and L2 were 12.7 mm and 8 mm, respectively. The reflection of the output coupling mirror was nearly 70% at 3.6 μm . The bandpass filter at 3.6 μm was used to filter out the residual pump sources. The pulse train was captured by a HgCdTe detector (PVI-4TE-5, VIGO System) and shown on a digital oscilloscope (MOD 3104, Tektronix) with 1 GHz bandwidth. The spectrum was measured by a Fourier spectrometer analyzer (Thorlab OSA207C).

3. Results and discussion

In the experiment, it was found that the output state of the 3.6 μm fiber laser was also pulsed when the repetition rate of the 976 nm pulse pump was at 386 Hz. However, it was gradually changed from pulse to CW mode when the repetition rate of the 976 nm pulsed pump was increased to 961 Hz, as shown in Fig. 2. It could be explained by the energy level structure of 3.6 μm Er:ZBLAN fiber laser, as shown in Fig. 3. The erbium ions at the ground state $^4I_{15/2}$ were pumped to the metastable level $^4I_{11/2}$ by the 976 nm pump source, and then they were pumped to the upper lasing level $^4F_{9/2}$ as a result of the 1973 nm pump source. The ions emitted laser radiation at 3.6 μm and relaxed from lower lasing level $^4I_{9/2}$ to $^4I_{11/2}$ via rapid multiple phonon decay. Due to the long energy level lifetime (6.8 ms) of the energy level $^4I_{11/2}$, the erbium ions could be stored at this energy level for a period of time. An additional 1973 nm photons could now repeat the process and elevate the ion again to the upper lasing level. The ions were cycled many times between the metastable level and the upper level before they decay back to the ground state. The main function of the 976 nm pump source was to provide enough erbium ions to the metastable energy level to meet the 1973 nm pumping demand. Therefore, under suitable pulse pumping, the CW output laser could also be achieved, as the ions stored on the metastable level would satisfy the requirements of 1973 nm pumping all the time.

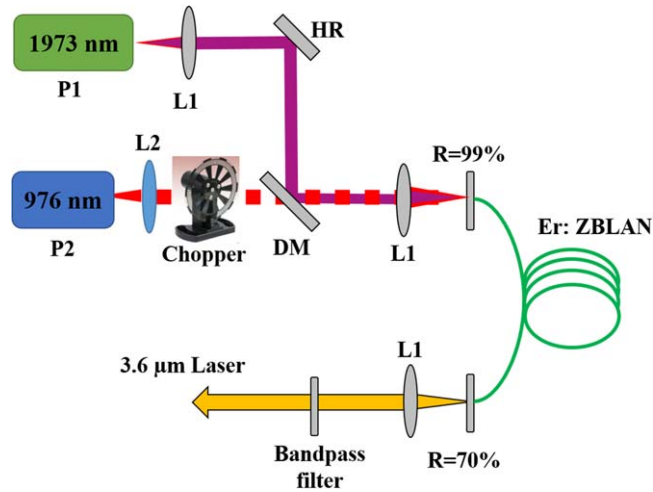


Fig. 1. (Color online) Schematic diagram of pulse pumping 3.6 μm Er:ZBLAN fiber laser. HR: high reflection mirror, DM: Dichroic mirror, L1, L2: Aspheric lens.

The output spectra of the CW and the pulse 3.6 μm fiber laser were also measured and compared, as shown in Fig. 4. The center wavelengths were all around 3.6 μm. There was only one peak for the CW laser, but five peaks for the pulse laser. For the pulse laser, the number of ions on the metastable $^4I_{11/2}$ level could not satisfy the requirements of 1973 nm pumping so that the number of ions on the upper lasing level $^4F_{9/2}$ or the lower lasing level $^4I_{9/2}$ would be changed accordingly. However, the excess or less population would lead to different sublevels of $^4I_{9/2}$ chosen.^{29,30} The multi-peak wavelengths emission might be caused by different sublevels of $^4I_{9/2}$.

In the experiment, it was found that the repetition rate and power of the 976 nm pump source were two main factors in the output state of 3.6 μm Er:ZBLAN fiber laser. The

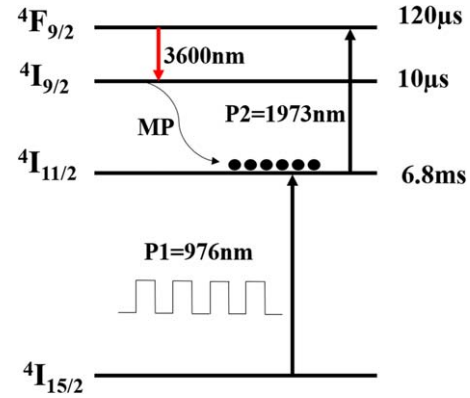


Fig. 3. (Color online) The energy level structure of 3.6 μm Er:ZBLAN fiber laser under pulse pumping.

boundary curves of the CW and pulse laser at different repetition rates and pump power were measured and plotted in Fig. 5. The boundary repetition rate from pulse to CW was decreased when the average power of 976 nm was increased from 1 to 1.5 W. This is because the ions pumped to the metastable level were increased under high pump power of 976 nm, which would meet 1973 nm pumping requirements. Meanwhile, the CW laser was also achieved by increasing the repetition rate of 976 nm. Increasing the repetition rate was equivalent to short the pump injection time interval. The ions at metastable level were consumed continuously by spontaneous emission and 1973 nm pump absorption. Reducing the pump injection interval would be useful to maintain the number of metastable ions at a relatively stable, which contributed to CW lasing. In addition, the laser was operated in the CW region at a low repetition rate of 976 nm by increasing the 1973 nm pump power. An additional 1973 nm photons could elevate more ions to the upper lasing level and the ions would be relaxed to metastable level rapidly. Due to

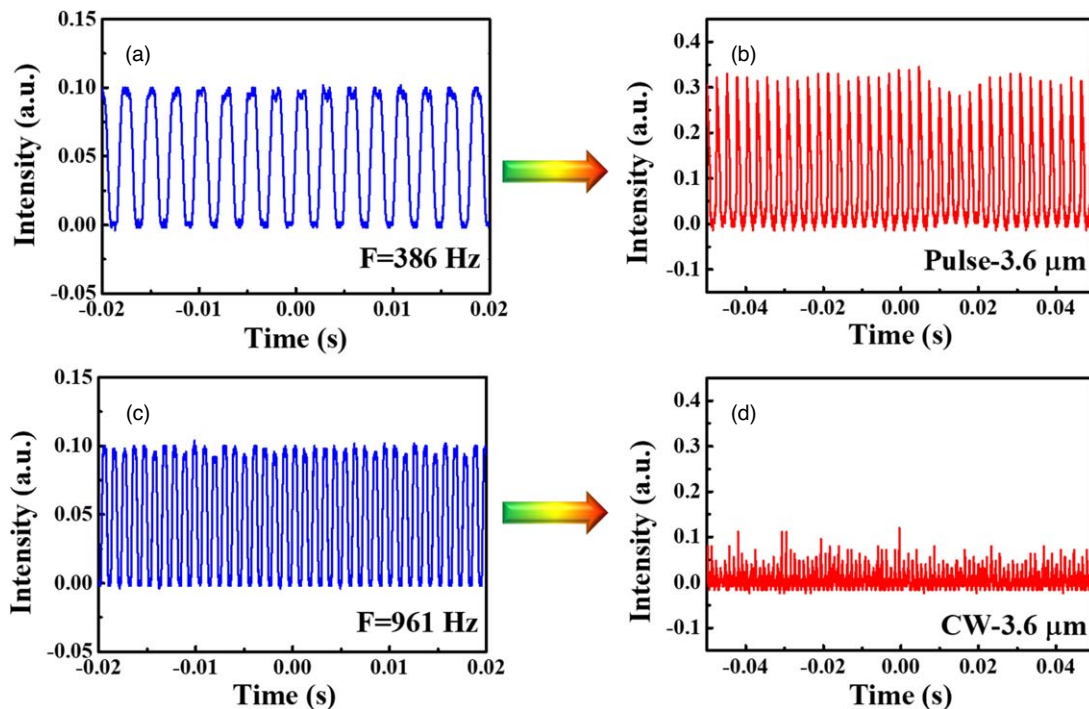


Fig. 2. (Color online) (a) 976 nm pulse train at a repetition of 386 Hz, (b) the temporal behavior of 3.6 μm Er:ZBLAN fiber laser at the 386 Hz pulse pumping, (c) 976 nm pulse train at a repetition of 961 Hz, (d) the temporal behavior of 3.6 μm Er:ZBLAN fiber laser at the 961 Hz pulse pumping.

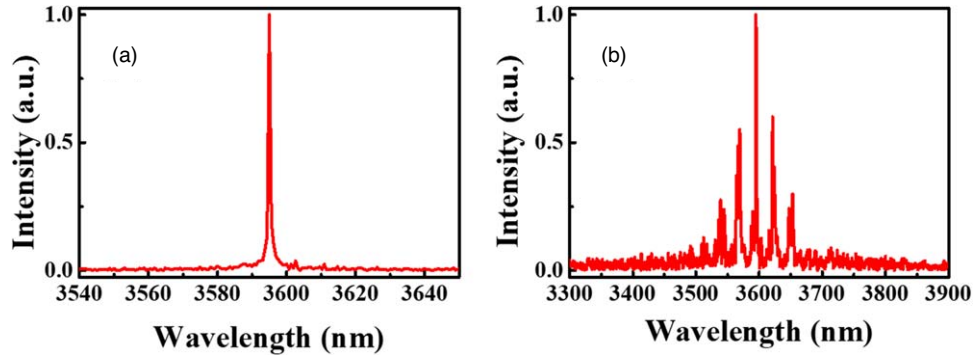


Fig. 4. (Color online) The spectra of the (a) CW and the (b) pulse 3.6 μm Er:ZBLAN fiber laser.

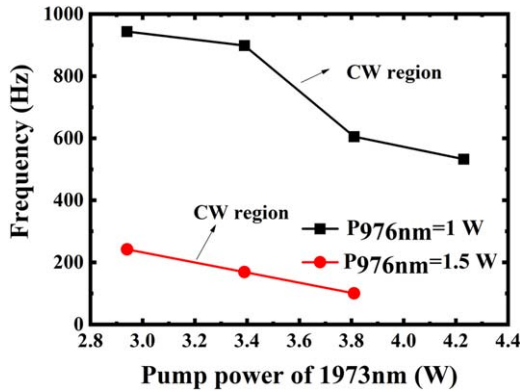


Fig. 5. (Color online) The region of CW 3.6 μm Er:ZBLAN fiber laser under pulse pumping.

the long lifetime (6.8 ms) of the metastable level, the cycled ions would be stored at this level to maintain the number of metastable ions. Therefore, increasing 1973 nm pump power also contributed to CW lasing at a low repetition rate of 976 nm.

Not only the output state but the output power of 3.6 μm Er:ZBLAN fiber laser was affected by pulse pumping. The output power curves at different 976 nm pumping repetition rates were compared and shown in Fig. 6. When the average power of the 976 nm pulsed pump source was 1 W, the output state changed from pulse to CW by increasing the repetition rate from 300 to 1000 Hz according to the Fig. 5, and the output power of the CW laser was also higher than

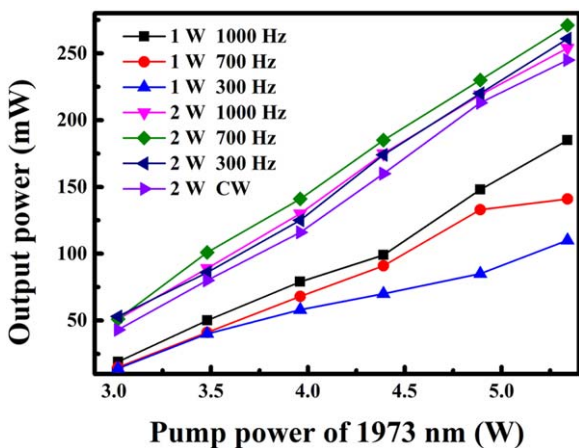


Fig. 6. (Color online) The output power curves of 3.6 μm Er:ZBLAN fiber laser at different repetition rate of 976 nm pump.

the pulse laser at the same pump power of 976 and 1973 nm. However, for the average power of 2 W for the 976 nm pump source, the output states of four cases were all CW lasers in Fig. 6. It was obvious that the output power was higher under pulse pumping compared with CW pumping, and the maximum output power curve was obtained with the repetition rate of 700 Hz. The maximum output power could be further improved by increasing the pumping power of 976 and 1973 nm.

In order to obtain a higher output power, actively water-cooled fiber chunks were used to hold the fiber to reduce the thermal damage and the unstable performance of the fiber laser induced by thermal-optical effects in the pumping end of the fiber. The output power curves of pulse pumping and CW pumping are compared in Fig. 7. The average powers of the 976 nm pump were 1.5 W, 2.5 W, 2.75 W and the repetition rates were all 700 Hz. The maximum output power of pulse pumping was 1.2 W under the average pump power of 2.5 W. Low average pump power (such as 1.5 W) would reduce the number of ions pumped to metastable level, which could not meet the 1973 nm pumping demand, leading to a decreased output power. However, excessive pump power (such as 2.75 W) would lead to output power roll-over, which might be caused by the wavelength switching,²⁸⁾ as shown in Fig. 8. The trends of output power curves were almost similar for 2.5 W pulsed and 3 W CW pumping at the low pump power of 1973 nm. However, the output power of pulse pumping was gradually higher than CW pumping with increasing the 1973 nm pump power. The pulse pumping

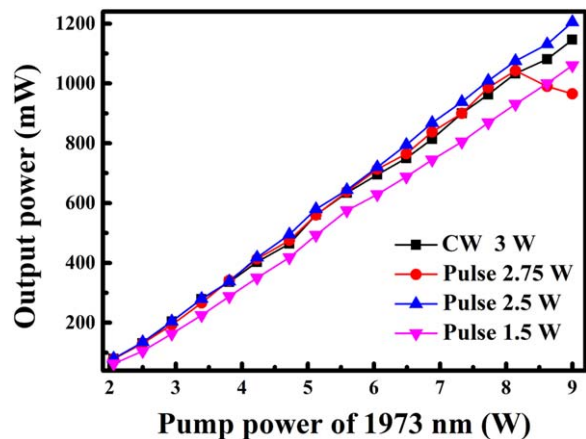


Fig. 7. (Color online) The output power curves of 3.6 μm Er:ZBLAN fiber laser under different pump power of 976 nm.

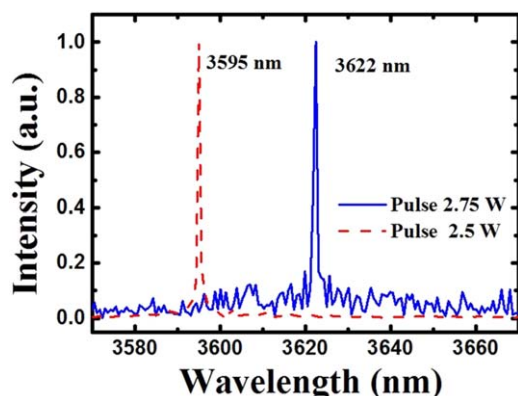


Fig. 8. (Color online) The output spectra under different 976 nm pulsed pump power (2.5 and 2.75 W) at the 1973 nm pump power of 9 W.

would be useful to reduce heat accumulation in the system so that the output power of pulse pumping was higher than CW pumping under high pump power. It can be seen that the power curve has not reached saturation. As the pump power increased, the advantages of pulse pumping become more prominent.

4. Conclusion

In summary, a 3.6 μm CW fluoride fiber laser was achieved by a combination of 976 nm pulse pumping and 1973 nm CW pumping. The output state could be changed from pulse to CW by increasing the pump power of 976 nm, the repetition rate of 976 nm and the pump power of 1973 nm. In order to achieve high output power, the repetition rate and pump power of pulse pumping was compared and optimized in the experiment. In addition, a 1.2 W output power of 3.6 μm CW fluoride fiber laser was achieved under the pulse pumping. The repetition rate and average pump power of 976 nm pulse pumping were 700 Hz and 2.5 W, respectively. Compared with CW pumping, pulse pumping could achieve higher output power under high pump power. Though limited by our homebuilt 1973 nm pump power, the demonstrated method provides a new solution for the realization of high power 3.6 μm fluoride fiber laser.

Acknowledgments

This work was supported by the National Natural Science Foundation of China (NSF) (Nos. 61790584), Independent Innovation project on State Key Laboratory of Luminescence and Applications (SKLA-Z-2021-07).

Disclosures

The authors declare no conflicts of interest.

- 1) K. Lsensee, N. Krogerliu, and W. Petrich, *Analyst* **143**, 5888 (2018).
- 2) H. Hazama, K. Ishii, H. Tsukimoto, and K. Awazu, *Newsroom* **2**, 1200801 (2014).
- 3) B. Ronald, I. K. Ilev, and I. Gannot, *Phil. Trans. R. Soc. Lond. A* **359**, 635 (2001).
- 4) B. Xiang, H. Yang, Y. Deyang, Z. Kuo, and C. Fei, *Infrared Laser Eng.* **49**, 20190512 (2020).
- 5) Y. Junyan, G. Faquan, L. Rui, and L. Gang, *Flight Control Detection* **3**, 34 (2020).
- 6) S. Affan, M. Mohsin, and S. Muhammad, *Defence Technol.* **17**, 583 (2021).
- 7) Z. Xiushan, Z. Gongwen, W. Chen, V. Leonid, W. Junfeng, T. Minghong, A. Robert, and N. Peyghamberian,, *J. Opt. Soc. Am. B* **34**, A15 (2017).
- 8) M. Jie, Q. Zhipeng, X. Guoqiang, Q. Liejia, and T. Dingyuan,, *Appl. Phys. Rev.* **6**, 021317 (2019).
- 9) R. Tingwei, W. Chunting, Y. Yongji, D. Tongyu, C. Fei, and P. Qikun, *Appl. Sci.* **11**, 11451 (2021).
- 10) V. Fortin, F. Maes, M. Bernier, S. Toubou, M. Dauteuil, and R. Vallee,, *Opt. Lett.* **41**, 559 (2016).
- 11) O. Henderson-Sapir, S. Jackson, and D. Ottaway, *Opt. Lett.* **41**, 1676 (2016).
- 12) M. Frédéric, V. Fortin, M. Bernier, and R. Vallee, *Opt. Lett.* **42**, 2054 (2017).
- 13) O. Henderson-Sapir, J. Munch, and D. Ottaway, *Opt. Lett.* **39**, 493 (2014).
- 14) F. Jobin, V. Fortin, F. Maes, M. Bernier, and R. Vallee, *Opt. Lett.* **43**, 1770 (2018).
- 15) O. Henderson, A. Malouf, N. Bawden, J. Much, S. Djachson, and D. Ottaway, *IEEE J. Sel. Top. Quantum Electron.* **23**, 0900509 (2017).
- 16) F. Maes, C. Stihler, L. Pleau, V. Fortin, J. Limpert, M. Bernier, and R. Vallee, *Opt. Express* **27**, 2170 (2019).
- 17) M. Lemieux, V. Fortin, T. Boilard, P. Paradis, F. Maes, L. Talbot, R. Vallee, and M. Bernier, *Opt. Lett.* **47**, 289 (2022).
- 18) L. Hongyu and W. Yongzhi, *J. Electron. Sci. Technol.* **20**, 100147 (2022).
- 19) L. Hongyu, Y. Jian, L. Fei, H. Zhu, X. Yao, Y. Fei, P. Hanlin, O. Francois, L. Jianfeng, and L. Yong,, *Opt. Express* **27**, 1367 (2019).
- 20) N. Bawden, H. Matsukuma, O. Henderson-Sapir, E. Klansataya, S. Tokita, and D. Ottaway,, *Opt. Lett.* **43**, 2724 (2018).
- 21) Y. Jian, L. Hongyu, L. Fei, L. Jianfeng, and L. Yong, *Photonics Technol. Lett.* **32**, 1335 (2020).
- 22) L. Hongyu and L. Jianfeng, *Chin. J. Laser* **49**, 0101003 (2022).
- 23) F. Zhiqiang, Z. Chunxiang, L. Jun, Y. Chen, and F. Dianyuan, *Opt. Laser Technol.* **14**, 107131 (2021).
- 24) H. Ting et al., *ACS Nano* **15**, 7430 (2021).
- 25) Q. Zhipeng et al., *Opt. Lett.* **47**, 890 (2022).
- 26) Q. Zhipeng, H. Ting, X. Guoqiang, M. Jingui, Y. Peng, Q. Liejia, L. Lei, Z. Liuming, and S. Deyuan, *Opt. Express* **26**, 8224 (2018).
- 27) N. Bawden, O. Henderson, S. Jackson, and D. Ottaway, *Opt. Lett.* **46**, 1636 (2021).
- 28) Q. Zhipeng, X. Guoqiang, M. Jingui, Y. Peng, and Q. Liejia, *Chin. Opt. Lett.* **11**, 61 (2017).
- 29) Z. Chunxiang, W. Jiandong, T. Pinghua, Z. Chujun, and W. Shuangchun, *IEEE Access* **7**, 147239 (2019).
- 30) W. Jincheng et al., *Chin. Opt. Lett.* **20**, 011404 (2022).